ARMY RESEARCH LABORATORY

A Multipurpose Projectile for Penetrating Urban Targets

by Robert A. Phillabaum II, Stephen J. Schraml, Richard L. Summers,
Brett R. Sorensen, Rayment E. Moxley, and James D. Cargile

ARL-RP-173   **April 2007**

NOTICES

Disclaimers

The findings in this report are not to be construed as an official Department of the Army position unless so designated by other authorized documents.

Citation of manufacturer's or trade names does not constitute an official endorsement or approval of the use thereof.

Destroy this report when it is no longer needed. Do not return it to the originator.

Army Research Laboratory
Aberdeen Proving Ground, MD 21005-5069

A Multipurpose Projectile for Penetrating Urban Targets

**Robert A. Phillabaum II, Stephen J. Schraml, Richard L. Summers,
and Brett R. Sorensen**
Weapons and Materials Research Directorate, ARL

Rayment E. Moxley and James D. Cargile
U.S. Army Corps of Engineers, ERDC

REPORT DOCUMENTATION PAGE

Form Approved
OMB No. 0704-0188

Public reporting burden for this collection of information is estimated to average 1 hour per response, including the time for reviewing instructions, searching existing data sources, gathering and maintaining the data needed, and completing and reviewing the collection information. Send comments regarding this burden estimate or any other aspect of this collection of information, including suggestions for reducing the burden, to Department of Defense, Washington Headquarters Services, Directorate for Information Operations and Reports (0704-0188), 1215 Jefferson Davis Highway, Suite 1204, Arlington, VA 22202-4302. Respondents should be aware that notwithstanding any other provision of law, no person shall be subject to any penalty for failing to comply with a collection of information if it does not display a currently valid OMB control number.
PLEASE DO NOT RETURN YOUR FORM TO THE ABOVE ADDRESS.

1. REPORT DATE *(DD-MM-YYYY)*	2. REPORT TYPE	3. DATES COVERED (From - To)
April 2007	Reprint	3 November 2003–23 September 2004

4. TITLE AND SUBTITLE	5a. CONTRACT NUMBER
A Multipurpose Projectile for Penetrating Urban Targets	
	5b. GRANT NUMBER
	5c. PROGRAM ELEMENT NUMBER

6. AUTHOR(S)	5d. PROJECT NUMBER
Robert A. Phillabaum II, Stephen J. Schraml, Richard L. Summers, Brett R. Sorensen, Rayment E. Moxley,[*] and James D. Cargile[*]	1L162618AH80
	5e. TASK NUMBER
	5f. WORK UNIT NUMBER

7. PERFORMING ORGANIZATION NAME(S) AND ADDRESS(ES)	8. PERFORMING ORGANIZATION REPORT NUMBER
U.S. Army Research Laboratory ATTN: AMSRD-ARL-WM-TC Aberdeen Proving Ground, MD 21005-5069	ARL-RP-173

9. SPONSORING/MONITORING AGENCY NAME(S) AND ADDRESS(ES)	10. SPONSOR/MONITOR'S ACRONYM(S)
	11. SPONSOR/MONITOR'S REPORT NUMBER(S)

12. DISTRIBUTION/AVAILABILITY STATEMENT

Approved for public release; distribution is unlimited.

13. SUPPLEMENTARY NOTES

[*]U.S. Army Corps of Engineers, Engineer Research and Development Center, CEERD-GM-I, 3909 Halls Ferry Rd., Vicksburg, MS 39180-6199

A reprint from the *Army Science Conference Proceedings*, Orlando, FL, 27 November 2006.

14. ABSTRACT

The U.S. Army Research Laboratory at the Aberdeen Proving Ground, MD is interested in developing a thin-walled munition capable of perforating an urban structure and delivering a payload intact to the interior of the structure. One of the most critical design aspects of this munition is the shell casing. Its shape, thickness, and material composition must be selected such that it has sufficient structural integrity to perforate a double-reinforced concrete wall as a rigid body and to deliver a payload to the interior of the structure.

A combined experimental-computational approach is being used to evaluate candidate munition configurations. The goal of maximizing the payload mass delivered, with a thin-walled and lightweight casing, must be balanced against the need to retain sufficient structural integrity to survive the breaching of the wall intact. In this study, various casing-wall thicknesses and nose shapes and their effects on the payload volume were considered.

15. SUBJECT TERMS

projectile, MOUT, PRONTO3D, Zapotec, caliber radius head, penetration

16. SECURITY CLASSIFICATION OF:			17. LIMITATION OF ABSTRACT	18. NUMBER OF PAGES	19a. NAME OF RESPONSIBLE PERSON Robert A. Phillabaum
a. REPORT UNCLASSIFIED	b. ABSTRACT UNCLASSIFIED	c. THIS PAGE UNCLASSIFIED	UL	12	19b. TELEPHONE NUMBER *(Include area code)* 410-278-6066

Standard Form 298 (Rev. 8/98)
Prescribed by ANSI Std. Z39.18

ii

A MULTIPURPOSE PROJECTILE FOR PENETRATING URBAN TARGETS

Robert A. Phillabaum II*, Stephen J. Schraml,
Richard L. Summers & Brett R. Sorensen

U.S. Army Research Laboratory
AMSRD-ARL-WM-TC
Aberdeen Proving Ground, MD 21005-5066

&

Rayment E. Moxley & James D. Cargile

Engineer Research and Development Center
U.S. Army Corps of Engineers
CEERD-GM-I
Vicksburg, MS 39180

ABSTRACT

The U.S. Army Research Laboratory at the Aberdeen Proving Ground, MD is interested in developing a thin-walled munition capable of perforating an urban structure and delivering a payload intact to the interior of the structure. One of the most critical design aspects of this munition is the shell casing. Its shape, thickness, and material composition must be selected such that it has sufficient structural integrity to perforate a double-reinforced concrete wall as a rigid body and to deliver a payload to the interior of the structure.

A combined experimental–computational approach is being used to evaluate candidate munition configurations. The goal of maximizing the payload mass delivered, with a thin-walled and lightweight casing, must be balanced against the need to retain sufficient structural integrity to survive the breaching of the wall intact. In this study, various casing-wall thicknesses and nose shapes and their effects on the payload volume were considered.

1. INTRODUCTION

Military Operations in Urban Terrain (MOUT) are becoming more prevalent in today's conflicts. The U.S. Army Research Laboratory (ARL) is studying the feasibility of designing a munition capable of perforating the exterior wall or roof of an urban structure and delivering its payload intact to the interior. Since 2003, ARL has been working on the development of a cannon-launched, thin-walled, multi-purpose projectile.

When used to defeat an urban structure, the multi-purpose projectile would be required to penetrate through to the interior of the structure and deliver its cargo. The structural integrity of the outer casing is integral to the success of the munition in this role. To this end, recent efforts have focused on the performance of candidate projectile nose shapes and casing-wall thicknesses in penetrating double-reinforced concrete (DRC) walls.

Numerical simulations are being conducted to support the development of the conceptual multipurpose munition. The simulations help to assess the projectile's structural dynamic response when penetrating concrete-wall targets. Simulations were performed using a variety of computational methods to guide design and to match a set of experiments.

The work described in this paper is part of an ongoing effort. Future computational work for the development of the projectile will likely address the evaluation of (1) additional geometries, (2) different component materials, (3) impact obliquity and velocity effects, and (4) penetration performance against other types of targets.

2. COMPUTATIONAL METHODS

Numerical simulations of the structural response of the projectile impacting concrete walls were performed with two computational tools. One of these is PRONTO3D, an explicit finite-element structural dynamics code (Taylor and Flanagan, 1989). In the PRONTO3D simulations described herein, loads applied to the exterior of the munition as a result of the penetration process were obtained from an analytical spherical cavity expansion (SCE) model implemented in PRONTO3D (Forrestal and Tzou, 1996). The input parameters for the cavity-expansion model are derived

from the mass, diameter, nose shape, and velocity of the penetrating body, and the density, compressive strength, and thickness of the concrete target. Thus, in the PRONTO3D simulations, the computational model consists only of the projectile body, with the exterior loads applied to the body via the analytical SCE model.

The other tool used in the computational studies is Zapotec (Bessette et al., 2003), a coupled Eulerian-Lagrangian code. As in the PRONTO3D simulations, the projectile components were represented in a Lagrangian finite-element model. However, the Zapotec simulations included the concrete target material in a surrounding Eulerian-computational mesh. Loading data between the Lagrangian projectile and the Eulerian target are exchanged via communication between the Eulerian and Lagrangian domains of the coupled simulation. In the Zapotec simulations, the concrete target material was modeled with a brittle fracture kinetics model (Silling, 1997).

The experiments included steel-reinforcing material (rebar). The rebar, however, was not represented in the Zapotec computational model of the target, nor was its effect explicitly included in the analytical modeling of loads applied to the projectile in the PRONTO3D simulations.

3. HEMISPHERICAL-NOSE PROJECTILE

To maximize payload capacity, a shape approximating a right-circular cylinder is desirable. However, this requires very heavy end caps to support gun launch and the interaction with the DRC wall. The mass of the end caps necessitates a shorter cylinder, thereby reducing the payload capacity. Previous research (Forrestal et al., 1994) has demonstrated that, for deep penetration into concrete targets, an ogive-nosed penetrator is more efficient and remains a rigid body at higher impact velocities than a blunt-nosed penetrator. However, the ogive-nose shape decreases the internal volume of the projectile in a length-constrained system and increases the likelihood of ricochet from an oblique impact. In addition, the DRC target of interest for this projectile is thin (less than 2 calibers thick) so penetration efficiency is not a driving factor. Consequently, the initial effort employed a hemispherical-nosed projectile.

3.1 Experiments

The hemispherical-nose projectiles used in the initial experiments were fabricated from Vascomax 300 maraging steel (Allvac, 2006). A photograph of this projectile is shown in Figure 1. Six projectiles were fabricated with a caliber radius head (CRH) of 0.5 (a hemispherical nose). Sand was used as a payload simulant in the projectiles. The projectiles were fired at impact velocities ranging from nominally 230 to 730 m/s into DRC walls at 0° obliquity. High-speed cameras were used uprange of the target face to determine the impact conditions. Cameras were also placed downrange of the target to obtain residual projectile velocities.
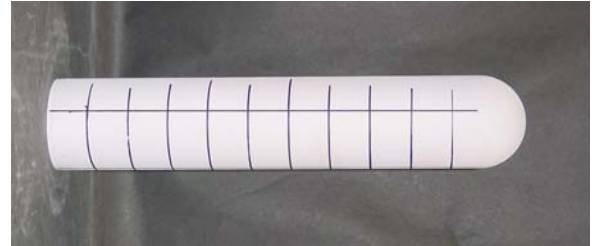

Figure 1. Photograph of the hemispherical-nose projectile.

A summary of the six experiments is given in Table 1. In each of the six experiments, the projectile perforated the DRC target. In the two highest velocity experiments, the projectile case failed catastrophically (Figures 2 and 3). Only slight deformation was observed on the recovered projectile from the 400-m/s experiment (Figure 4), at the location where the nose blends into the case diameter. In the other three experiments (304 m/s and less), no projectile deformation was observed.

Table 1. Summary of the CRH=0.5 experiments.				
Projectile	Striking Velocity (m/s)	Total Yaw (degrees)	Residual Velocity (m/s)	Projectile Integrity Remarks
CRH 0.5	232	8.3	133*	Intact
CRH 0.5	300	No Data	231*	Intact
CRH 0.5	304	0.9	235	Intact
CRH 0.5	400	0.7	313	Slight deformation
CRH 0.5	529	1.9	423*	failed
CRH 0.5	721	0.3	535*	failed
				*Concrete debris velocity

In these experiments, debris from the target made it difficult to see the projectile exiting the target, complicating the estimation of the residual projectile velocity. This was especially true for the high-velocity impact experiments in which the projectile failed. For these cases, the residual velocities were obtained by tracking the motion of the debris field, assuming that the projectile was inside the debris field and traveling at approximately the same velocity.

Figure 2. Photograph of the recovered CRH=0.5 projectile pieces from the 529-m/s experiment.
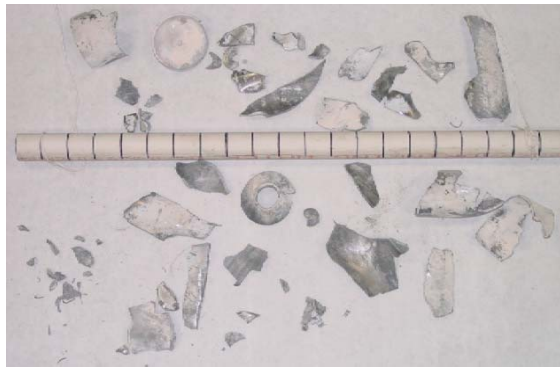

Figure 3. Photograph of the recovered CRH=0.5 projectile pieces from the 721-m/s experiment.
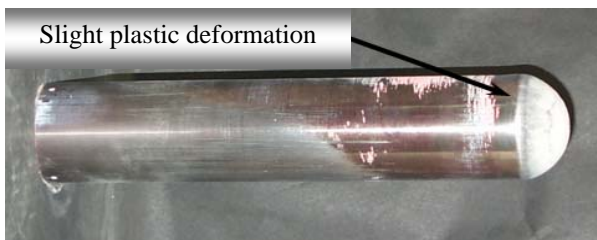

Slight plastic deformation

Figure 4. Photograph of the recovered CRH=0.5 projectile from the 400-m/s experiment.

3.2 Numerical Simulations

A series of numerical simulations was performed with PRONTO3D and Zapotec in an attempt to determine the cause of the structural failure of the projectiles. A set of PRONTO3D simulations was performed with impact velocities matching those measured in the experiments. In an attempt to identify a means to determine the structural integrity of follow-on configurations, an analysis of the simulation results—based upon the experimental observations— was performed. The analysis of the simulation results consisted of tracking the maximum von Mises stress and maximum equivalent plastic strain in the case material as

a function of time, regardless of where in the case the maximum value may occur at any given time. The results of this analysis are presented in Figure 5. The plot on the left of the figure shows the maximum von Mises stress in the case normalized by the yield strength of the case material (2.1 GPa, 300 ksi) as a function of time during the penetration event. The plot on the right of Figure 5 shows the maximum equivalent plastic strain in the case as a function of time.

The stress and strain histories from impact events of varying velocities have different characteristic time scales, making it difficult to compare them directly. For the purpose of comparison, the time scales from the maximum stress and strain histories were divided by the time required for the projectile to travel a predetermined distance. The resulting maximum case stress and strain histories are plotted in Figure 5 as a function of "event time," in which event time equal to 1 is the time required for the projectile to travel the predetermined distance.

The case maximum normalized von Mises stress in the left plot of Figure 5 reveals that for the 232-m/s impact, the stress in the case is always in the elastic region. For the 300-m/s simulation, the maximum von Mises stress in the case reaches the yield stress for only two short periods. For the 400-m/s impact, the maximum stress is at the yield state for much of the event. Finally, for the 529-m/s and 721-m/s simulations, the maximum von Mises stress in the case rises to the yield state immediately after impact and remains there for the duration of the event.

From the maximum case von Mises stress plot alone, one cannot reliably assess the structural integrity of the case in these impact events. However, in the maximum case equivalent plastic strain histories in the right-hand plot of Figure 5, there is a clear correlation between the maximum strain histories and the experimental observations. The two lowest-impact velocities produced no noticeable deformation of the projectiles and the corresponding maximum strain histories show no significant deformation. For the 400-m/s simulation, the maximum strain reaches a maximum of approximately 2.9%, less than the failure strain from the material characterization and in qualitative agreement with the modest deformation observed in the experiment. At the impact velocities of 529 and 721 m/s, the case maximum equivalent plastic strain exceeds the quasistatic failure strain denoted by the dashed line at 10.4%. This resulted in the catastrophic structural failure that was observed in the experiments. It should be noted that the quasistatic failure strain from the material characterization is not the same strain at which one would expect the case to fail under dynamic loading. Instead, it is used here as an indicator of structural integrity and not an absolute
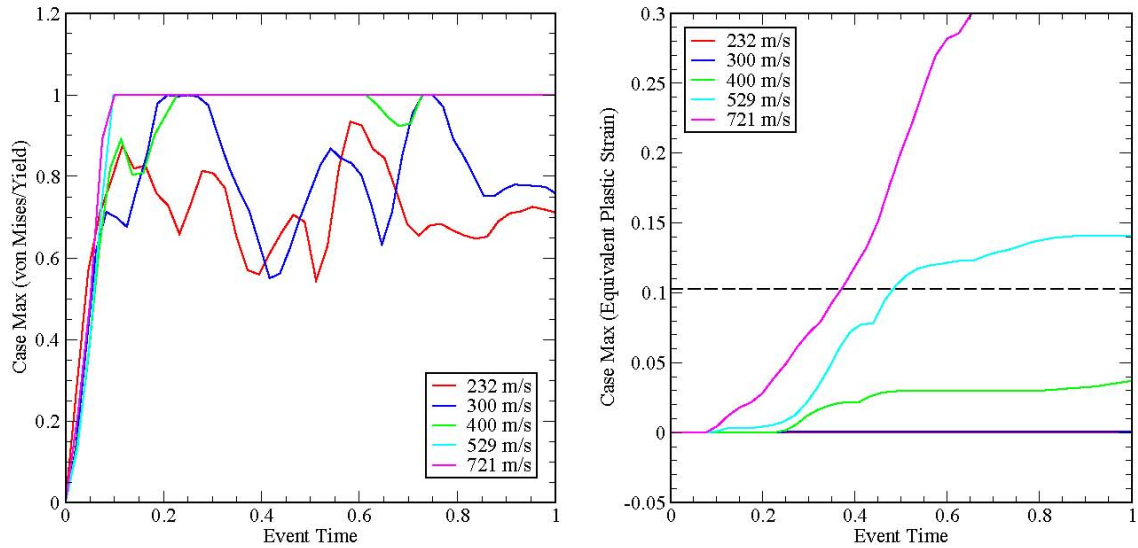
3

Figure 5. CRH=0.5 projectile case maximum stress and strain histories.

measure.

Zapotec simulations were run for impact velocities at which either noticeable deformation or destruction of the projectile was observed (400, 529, and 721 m/s). The results of these simulations are provided in Figure 6. As previously stated, there is no rebar present in the target model. Event histories of the maximum case equivalent plastic strain from the three Zapotec simulations are compared to the corresponding PRONTO3D simulations in the plot of Figure 6. In this plot, the solid lines represent the PRONTO3D results (plotted previously in Figure 5) and the dashed lines represent the Zapotec simulation results. For the 400-m/s simulation, the maximum case equivalent plastic strain reaches a steady value of approximately 1.5%, less than the PRONTO3D result of approximately 2.9%. Similarly, the Zapotec simulation produces a lower late-time maximum strain than the corresponding PRONTO3D simulation for the 529-m/s simulation. However, for the highest impact velocity the Zapotec simulation produces a greater late-time case maximum strain than PRONTO3D (40% as compared to 34%), but both are well above the quasistatic failure strain of the case material. Despite these differences between the two sets of simulations, both are useful in assessing the structural integrity of the case when compared to the experimental results.

The deformations predicted in the Zapotec simulations agree qualitatively with the observed experimental-projectile deformations. The 529-m/s Zapotec simulation produced the greatest deformation in the region where the nose blends into the case wall. This is consistent with observations of the recovered projectile from the experiment performed with a striking velocity of 400 m/s. In this experiment, plastic deformation (bulging) of the case is only evident where the nose blends into the case wall (Figure 4). In addition, the

recovered pieces of the projectile from the 529-m/s striking velocity test (Figure 2) indicate the projectile began to fail near the blend between the nose and the shank of the projectile. The 721-m/s Zapotec simulation predicts large regions of high strain, indicating that much of the case is beyond the failure criteria. This result is verified by the photograph of the projectile from the 721-m/s experiment (Figure 3) in which the case broke into many small pieces.
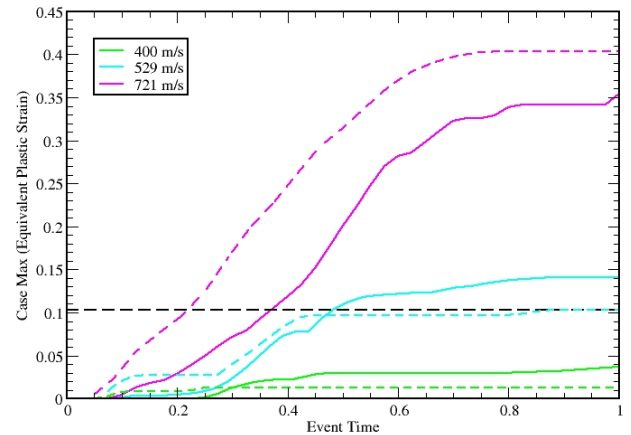

Figure 6. Simulation results for CRH=0.5 projectile impacting concrete wall.

4. OGIVE-NOSE PROJECTILE

Because the hemispherical-nose projectile case failed during high-velocity impact, it was necessary to explore alternative case configurations to improve structural integrity. The numerical simulations indicated that the weakest part of the projectile was in the nose

4

region. Consequently, an alternative configuration using an ogive (CRH=2) nose shape was studied computationally to determine its penetration performance and ability to resist structural failure at the higher velocities. The CRH=2 projectile configuration retained the same overall projectile length and wall thickness as the CRH=0.5 configuration. The resulting mass of the CRH=2 configuration is 8% lower than the CRH=0.5 configuration.

4.1 Computational Verification of CRH=2 Design

Numerical simulations were performed to assess the structural response of the CRH=2 projectile configuration when subjected to loads resulting from penetration of the concrete target at the same velocities studied for the CRH=0.5 configuration. The results of these simulations are summarized in Figure 7, which is an event history plot of the maximum equivalent plastic strain in the CRH=2 case for impact velocities of 400, 529, and 721 m/s. This plot demonstrates that the CRH=2.0 nose shape produces strain levels in the case that are below the quasistatic failure strain at the highest velocity considered. From these results, one might conclude that the change in nose shape from CRH=0.5 to CRH=2 significantly improved the structural integrity of the projectile for normal impact with concrete-wall targets at high velocity.
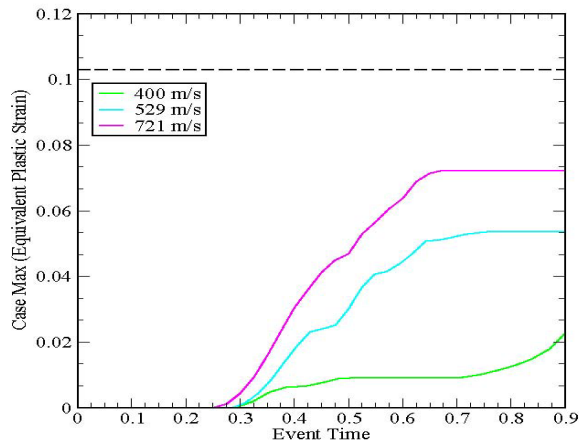

Figure 7. CRH=2 projectile simulation results.

4.2 CRH=2 Projectile Experiments

The CRH=2 projectiles used in the second set of experiments were also fabricated from Vascomax 300 maraging steel. A photograph of the CRH=2 projectile is shown in Figure 8. Two projectiles were fired against 0° DRC walls at velocities of 707 m/s and 784 m/s. In both experiments the projectiles exited the DRC wall intact

(Figures 9 and 10). A summary of the two CRH=2 experiments is given in Table 2.

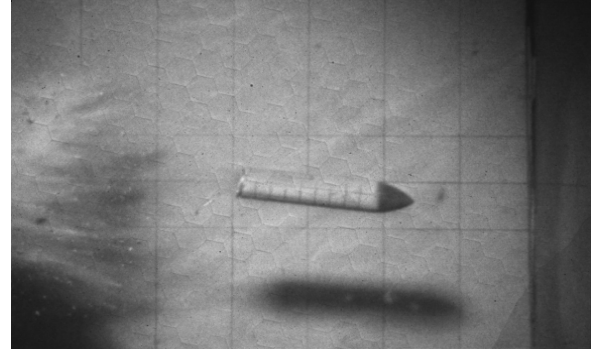Figure 8. Photograph of the CRH=2 projectile.

Figure 9. High-speed camera image of the CRH=2 projectile after exiting the DRC target in the 707-m/s experiment.
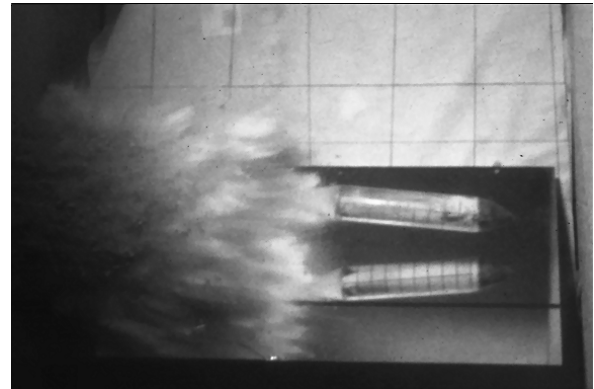

Figure 10. High-speed camera image of the CRH=2 projectile after exiting the DRC target in the 784-m/s experiment.

Table 2. Summary of the CRH=2 experiments.

Projectile	Striking Velocity (m/s)	Total Yaw (degrees)	Residual Velocity (m/s)	Remarks
CRH 2	707	0.8	634	Intact
CRH 2	784	3.1	719	Intact

4.3 Residual Velocities

The residual velocities from the experiments with the CRH=0.5 projectile configuration are compared to those of the simulation in Figure 11. This figure shows that the simulation of the CRH=0.5 configuration closely follows the experimental results for impact velocities of 400 m/s and greater. The CRH=0.5 simulation results fall below the experimental results at the lower impact velocities, indicating that the simulation would predict a slightly higher limit velocity for this target than the experiments suggest.
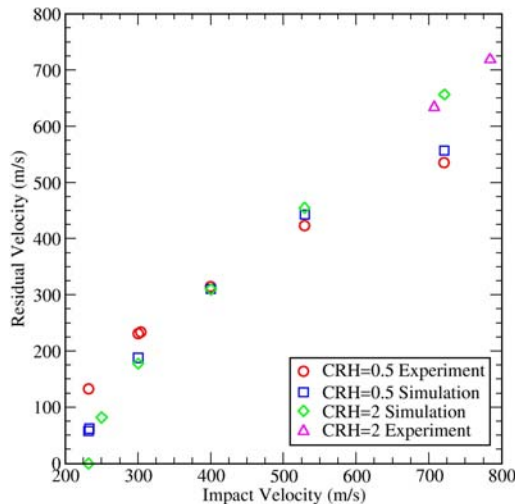
Figure 11. Residual velocities for CRH=0.5 and CRH=2.0 nose shapes.

The residual velocity results of the CRH=2 simulations and experiments are also plotted in Figure 11. These results reveal that the predicted limit velocity of the CRH=0.5 configuration is lower than the CRH=2 configuration against the DRC wall. This is a result of the lower projectile mass of the CRH=2 configuration as compared to the CRH=0.5 configuration. In normal (0° obliquity) impacts at higher impact velocities, the CRH=2 configuration has a greater residual velocity because it is a more efficient penetrator than the blunt-nose CRH=0.5 configuration.

5. SUMMARY

A combined experimental-computational approach has been taken to demonstrate that a thin-wall projectile can successfully perforate a DRC target as a rigid body. The approach demonstrates a robustness criterion that is dependent upon the delivery velocity. From the limited data presented, it can be seen that nose design is a very important criterion for a thin-walled projectile to survive penetration of a thin-slab concrete wall.

REFERENCES

Allvac, "VascoMax C-200/C-250/C-300/C-350 Technical Data Sheet," 2000, ATI Properties, Inc., Sept. 2006 <http://www.allvac.com/allvac/pages/PDF/tech/Vas coMaxC.pdf>.

Bessette, G.C., R.L. Bell, R.A. Cole, C.T. Vaughan, L. Yarrington, and S.W. Attaway. "Zapotec: A Coupled Eulerian-Lagrangian Computer Code, Methodology and User Manual, Version 1.0. SAND2003-3097, Sandia National Laboratories, Albuquerque, NM, October 2003.

Forrestal, M. J., B. S. Altman, J. D. Cargile, and S. J. Hanchak. "An Empirical Equation for Penetration Depth of Ogive-Nose Projectiles into Concrete Targets." Int. J. Impact Energy Vol. 15, No.4, pp 395-405, 1994.

Forrestal, M.J. and D.Y. Tzou. "A Spherical Cavity Expansion Penetration Model for Concrete Targets." International Journal of Solids Structures, 1996.

Silling, S.A. "Brittle Fracture Kinetics Model for Concrete." SAND97-0439C, Sandia National Laboratories, Albuquerque, NM, July 1997.

Taylor, L.M and D.P. Flanagan. "PRONTO3D: A Three-Dimensional Transient Solid Dynamics Program." SAND87-1912, Sandia National Laboratories, Albuquerque, NM, March 1989.

NO. OF
COPIES   ORGANIZATION

1   DEFENSE TECHNICAL
(PDF   INFORMATION CTR
ONLY)   DTIC OCA
         8725 JOHN J KINGMAN RD
         STE 0944
         FORT BELVOIR VA 22060-6218

1   US ARMY RSRCH DEV &
         ENGRG CMD
         SYSTEMS OF SYSTEMS
         INTEGRATION
         AMSRD SS T
         6000 6TH ST STE 100
         FORT BELVOIR VA 22060-5608

1   DIRECTOR
         US ARMY RESEARCH LAB
         IMNE ALC IMS
         2800 POWDER MILL RD
         ADELPHI MD 20783-1197

3   DIRECTOR
         US ARMY RESEARCH LAB
         AMSRD ARL CI OK TL
         2800 POWDER MILL RD
         ADELPHI MD 20783-1197

         ABERDEEN PROVING GROUND

1   DIR USARL
         AMSRD ARL CI OK TP (BLDG 4600)

ABERDEEN PROVING GROUND

23   DIR USARL
      AMSRL WM EG
        J SMITH
        T ROSENBERGER
      AMSRL WM EG
        E SCHMIDT
      AMSRL WM T
        P BAKER
        A CARDAMONE
      AMSRL WM TB
        J COLBURN
        R BANTON
      AMSRL WM TC
        R COATES
        G BOYCE
        T FARRAND
        M FERMEN-COKER
        E KENNEDY
        K KIMSEY
        R PHILLABAUM (2 CPS)
        D SCHEFFLER
        S SCHRAML (2 CPS)
        B SORENSEN (2 CPS)
        R SUMMERS (2 CPS)
        A TANK